SELF-PROPELLED WAKES AT DIFFERENT FROUDE NUMBERS IN A STRATIFIED FLUID

Matthew B. de Stadler[1] and Sutanu Sarkar[2]
Mechanical and Aerospace Engineering Department
University of California San Diego
9500 Gilman Drive #0411, La Jolla, CA 92093
mdestadl@ucsd.edu[1], sarkar@ucsd.edu[2]

ABSTRACT

Direct numerical simulation is used to study the evolution of a self-propelled, temporally evolving, wake in a stratified fluid at three different Froude numbers: 3, 10, 20. At higher Froude number the wake was found to decay faster resulting in decreased values of mean and turbulent statistics such as the defect velocity, mean kinetic energy, turbulent kinetic energy, and turbulence intensities, and increased wake dimensions at equivalent Nt, where N is the buoyancy frequency. Despite large quantitative differences between cases, transition between flow regimes was found to occur at comparable Nt. A significant increase in both the relative contribution and absolute value of the cross-stream component of the mean kinetic energy was observed as a result of the collapse in the vertical direction from $3 < Nt < 30$ in the higher Froude number cases. Different scaling was observed for mean and turbulent statistics which shows that self-similarity is not valid. Consistent mean velocity and vertical vorticity structure were observed between cases despite significant differences in turbulent kinetic energy structure.

INTRODUCTION

Direct numerical simulation (DNS) is used to study the wake behind an axisymmetric self-propelled body in a stratified fluid. A body moving under its own power with a jet propulsor has a near wake velocity profile characterized by a doubly-inflected mean profile with both thrust and drag lobes as shown in Figure 1. The special case of a body moving at constant speed results in a near wake with zero net momentum, also called a momentumless wake. The wake is known to be sensitive to the Reynolds number, $Re = UD/\nu$ where U is the velocity of the body D is the diameter of the body and ν is the kinematic viscosity, and Froude number, $Fr = U/ND$, where $N = (-(g/\rho_0)\partial\rho/\partial x_3)^{1/2}$ is the buoyancy frequency.

Stratified turbulent wakes have been studied extensively, see Lin & Pao (1979) for near wake scaling laws for self-propelled bodies, Riley & LeLong (2000) for wakes with strong stratification, and Spedding (1997), Diamessis *et al.* (2011) and references therein for a discussion of wakes at high Froude number. Important for the current study, the stratified wake evolution model proposed by Spedding (1997) of a near wake region (NW) where the wake evolves as though unstratified, a non-equilibrium regime (NEQ) where the wake adjusts to buoyancy effects with a reduced decay rate of turbulent kinetic energy followed by a quasi-2D regime (Q2D) where motion is primarily in the horizontal plane, has been found to be appropriate, subject to minor modifications, for both towed, Diamessis *et al.* (2011), and self-propelled wakes, Brucker & Sarkar (2010). Recently, self-propelled wakes studies have been performed experimentally by Meunier & Spedding (2006), and numerically by Chernykh *et al.* (2009), Brucker & Sarkar (2010). With the exception of the recent DNS study of Brucker & Sarkar (2010), all previous simulations of a self-propelled body have employed turbulence models, see Chernykh *et al.* (2009) for a list of the relevant papers. de Stadler *et al.* (2010) used DNS to study the effect of Prandtl number on a stratified turbulent wake and found qualitatively similar behavior at $Pr = 7$ and $Pr = 1$ validating the use of $Pr = 1$ in numerical simulations.

The present study is designed to investigate the effect of Froude number on the evolution of a self-propelled wake. To the best of the authors' knowledge, this is the first study focusing on Froude number effects beyond the NW region for a self-propelled wake in the open literature as well as the first study to use DNS for this purpose. We are interested in assessing (1) The effect of Fr on characteristic velocity and length scales, (2) The effect of Fr on mean and turbulent kinetic energy and associated budgets, (3) The effect of Fr on flow structure for the streamwise velocity, turbulent kinetic energy, and vertical vorticity.

FORMULATION

The formulation of this study is equivalent to that used by de Stadler *et al.* (2010), see that reference for details. Briefly, we consider the case of a body of size D moving at steady velocity U in a linearly stratified fluid as shown in Figure 1. The wake is simulated from the near wake to the far wake using the temporal approximation, statistics in the temporal case can be related to the spatially evolving case by the relation $x = x_0 + Ut$ where $x_0 = 6$ is the spatial location corresponding to the initial conditions and t is the time elapsed in the simulation. DNS is used to solve the three-dimensional,

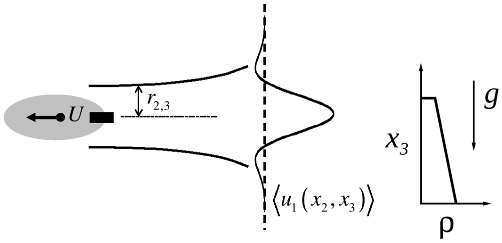

Figure 1: Problem formulation.

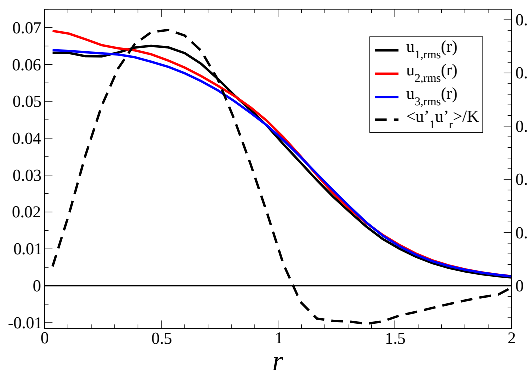

Figure 2: Initial conditions at the beginning of the simulations. The left axis is for the $u_{i,rms}$ terms and the right axis is for $\max(< u_1' u_r' > /K)$.

unsteady, incompressible, Navier-Stokes equations subject to the Boussinesq approximation. A finite volume method employing a staggered grid formulation with the velocities at cell faces and scalars at the cell centers is used. Time advancement is performed using a low storage third-order Runge-Kutta scheme and spatial derivatives are discretized using second order centered differences. Boundary conditions are taken to correspond to an undisturbed background fluid; stress-free boundary conditions are applied for the velocity in x_2 and x_3, the background density gradient is applied at the x_3 boundaries and $\partial\rho/\partial x_2 = 0$ at the x_2 boundaries. By definition, in the temporal approximation all variables are periodic in x_1.

Simulations are initialized using the initial mean profile of Rottman *et al.* (2003).

$$u_{SP}(r) = U_0\left[1 - \frac{1}{2}\left(\frac{r}{r_0}\right)^2\right]\exp^{-\frac{1}{2}\left(\frac{r}{r_0}\right)^2},$$

where $U_0 = 0.11$ and $r_0 = 0.5$. Turbulent fluctuations are added with a given spectrum, $E(k) = (k/k_0)^4 \exp^{-2(k/k_0)^2}$ where $k_0 = 4$ and then cropped to the wake using $g(r) = (1 + r^2/r_0^2)\exp^{-r^2/2r_0^2}$, where $a = 0.055$ is the maximum initial amplitude of the velocity fluctuations. The initial velocity profile is then allowed to adjust following the unstratified Navier-Stokes equations with the mean profile held constant until $\max(< u_1' u_r' > /K) \approx 0.25$ where $K = u_i' u_i'/2$ is the turbulent kinetic energy. One of the advantages of the current study is that we are able to enforce identical initial conditions between cases such that the only parameter varying is the Froude number. As noted by Meunier & Spedding (2006), the self-propelled momentumless wake is highly sensitive to initial conditions which poses difficulty for experimentalists.

Table 1: Simulation parameters. Note that part 1 uses stretching with parameters: $l_2 = 3.4$, $l_3 = 1.8$, $\min(\Delta x) = 0.0171$, $n_{2,b} = n_{3,b} = 25$, $pc_2 = 1.0059$, $pc_3 = 1.0065$. Parts 2 and 3 use uniform grids.

	L_1	L_2	L_3	n_1	n_2	n_3
part 1	48.13	22.35	10.22	2816	896	512
part 2	48.13	33.63	16.13	1408	1024	512
part 3	48.13	33.54	16.24	640	512	256

Simulation parameters

Simulations were performed at a fixed Reynolds number of 25,000 and Prandtl number of 1 at three different Froude number values: 3, 10, 20. Each simulation was run from the near wake, $x_0 = 6$, until the far wake, $Nt = 400$. Simulations were designed for a resolution of $\Delta x/\eta < 4$. To reduce computational costs, the simulations are re-gridded when $\Delta x/\eta < 1$ onto a grid with half the resolution in each direction. The grid parameters are given in Table 1, explanations for the variables are given in de Stadler *et al.* (2010).

The $Fr = 3$ case required 3,400 CPU hours, 3,000 for the first part, $6 < t < 285$, and 400 for the second part, $285 < t < 1279$. The $Fr = 10$ case required 2,325 CPU hours, 1,900 for the first part, $6 < t < 140$, 350 for the second part, $140 < t < 744$, and 75 for the third part, $744 < t < 4937$. The $Fr = 20$ case required 2,160 CPU hours, 1,750 for the first part, $6 < t < 143$, 250 for the second part, $143 < t < 697$, and 160 for the third part, $697 < t < 8473$. Each case required an additional 20% increase in CPU time to ensure that re-gridding did not introduce undue errors.

CHARACTERISTIC WAKE SCALES

As shown in Figure 3(a), the evolution of the defect velocity, U_0, at different Froude numbers shows significant differences when plotted versus the time evolution. At higher Froude number, the onset of buoyancy effects is delayed and the wake decays in a manner more consistent with an unstratified wake with reduced values of the defect velocity and transition between flow regimes occurring at a later time. Statistics generally overlap in the first few time intervals with the $Fr = 3$ data diverging at $t \approx 8.5$, and $Fr = 10$ diverging after $t \approx 20$. However, by plotting the wake in terms of buoyancy timescales elapsed, Nt, it is seen that each Fr case exhibits a change in slope at $Nt = 2 \sim 3$ in Figure 3(b). Note that all plots in this paper scaled by Nt are offset by 1 so that data can be viewed on a logarithmic scale. Also note that by plotting data against Nt removes the initial overlap region between multiple cases that occurs when data is plotted against t. For $Nt < 2$, there is no evidence that there is an unstratified momentum wake power law, $t^{-2/3}$, nor is there evidence of an unstratified momentumless wake power law, $t^{-4/5}$. This is

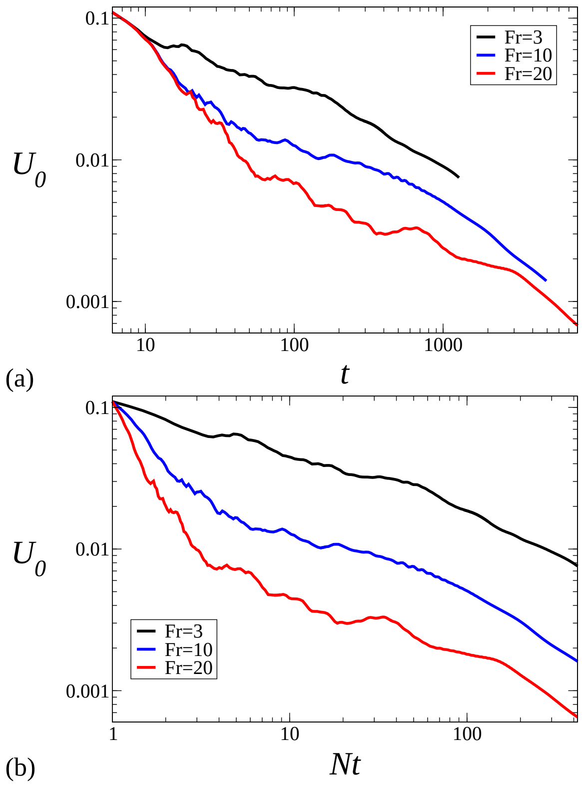

Figure 3: Defect velocity. (a) Unscaled. (b) Normalizing the wake evolution by the buoyancy timescale Nt.

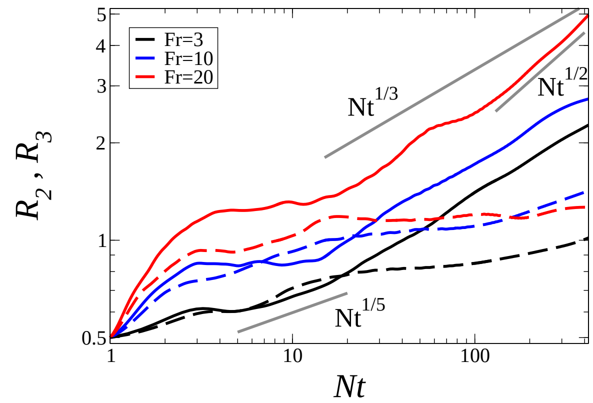

Figure 4: Wake width (solid lines) and wake height (dashed lines).

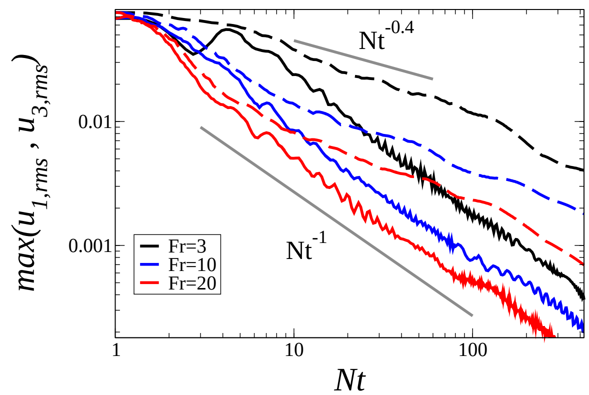

Figure 5: Maximum value of rms velocities $u_{1,rms}$ and $u_{3,rms}$. $u_{1,rms}$ is shown with dashed lines and $u_{3,rms}$ is shown with solid lines.

at odds with the towed wake results of Spedding (1997) who found $t^{-2/3}$ scaling at early time in a towed wake. Note that neither $U_0 Fr^{2/3}$ nor $U_0 Fr^{4/5}$, when used instead of U_0, removes differences among the different cases in their Nt evolution.

There have been a number of possible definitions proposed for determining the wake dimensions for a self-propelled wake, the second order spatially centered moment based on the mean streamwise velocity of Brucker & Sarkar (2010) was adopted for this study with

$$R_\alpha^2(t) = F\frac{\int_A (x_\alpha - x_\alpha^c)^2 \langle u_1 \rangle^2 \, dA}{\int_A \langle u_1 \rangle^2 \, dA}, \quad (1)$$

$$x_\alpha^c(t) = \frac{\int_A x_\alpha \langle u_1 \rangle^2 \, dA}{\int_A \langle u_1 \rangle^2 \, dA},$$

where $F = 2$ is a normalization factor to set the initial wake width, R_2, and height, R_3, to 0.5, and A is the area of the $x_2 - x_3$ plane not including the sponge region. As shown in Figure 4, the wake width and height evolve in a qualitatively similar manner between cases. The wake begins by expanding in the horizontal direction and then has a period of approximately constant width followed by growth with a power law $Nt^{1/3}$. At increased Froude number, the wake has expanded further at all times. In the $Fr = 20$ case the late wake growth rate has increased to $Nt^{1/2}$ which is commensurate with late time expansion due to viscous diffusion. Meunier & Spedding (2006) also observed an increase in the growth rate of the wake width around $Nt = 100$ for their $Re = 25{,}000, Fr = 20$ slender spheroid case.

Evidence of the accelerated collapse region appears in R_3 where the initial wake growth rate drops around $Nt = 3$. The wake height then increases as $Nt^{1/5}$ until $Nt \approx 20$ after which remains approximately constant during the NEQ regime before growing at late time with as $Nt^{1/5}$. The $R_2 \sim Nt^{1/5}$ scaling laws is consistent with the length scale scaling obtained from similarity analysis for a momentumless wake in an unstratified fluid. This value is similar to the $Nt^{1/4}$ scaling observed by Lin & Pao (1979) at early time for the wake height and it matches the value obtained by Brucker & Sarkar (2010) for $Nt < 30$. As with the wake width, the wake height increases at equivalent Nt with increased Froude number.

Measuring the turbulence in a stratified wake experiment is difficult and simple diagnostics such as the maximum value of the rms of velocity components have been used to attempt to characterize the turbulence. As found by Brucker & Sarkar (2010) and Lin & Pao (1979), the maximum values of $u_{1,rms}$ and $u_{3,rms}$ show a clear asymmetry with the vertical velocity fluctuations decaying significantly faster than the streamwise velocity fluctuations as shown in Figure 5. $u_{3,rms}$ was found to scale as Nt^{-1} and $u_{1,rms}$ as $Nt^{-0.4}$ in the NEQ regime.

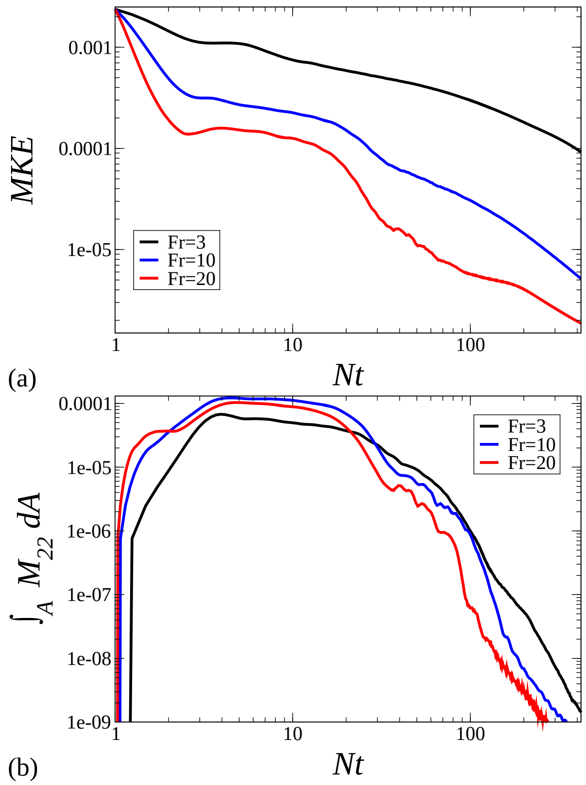

Figure 6: (a) Integrated mean kinetic energy. (b) M_{22} component of MKE.

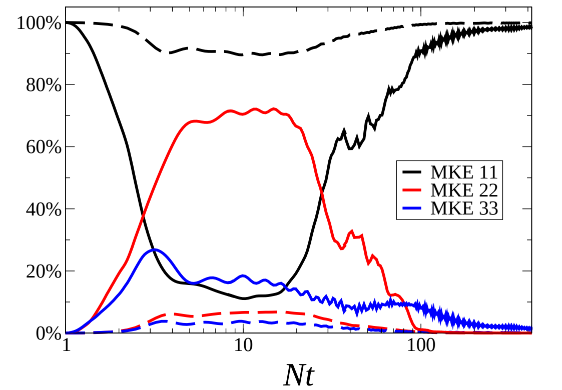

Figure 7: Breakdown of mean kinetic energy into directional components. (Dashed lines) $Fr = 3$. (Solid lines) $Fr = 20$.

ENERGETICS

In addition to characteristic scales such as the defect velocity, one can also investigate integrated quantities such as the integrated mean kinetic energy, $MKE = \int_A \langle u_i \rangle \langle u_i \rangle /2\,dA$. The mean kinetic energy shows clear differences between cases as shown in Figure 6 with the higher Froude number cases experiencing a longer lasting plateau of MKE from $3 < Nt < 30$ at early time as well what appears to be a different flow regime in between the NEQ and Q2D regimes. The difference in the wake evolution between $3 < Nt < 30$ in the $Fr = 10$ and $Fr = 20$ cases occurs due to a large increase in the $M_{22} = \langle u_2 \rangle \langle u_2 \rangle /2$ component of the mean kinetic energy. As shown in Figure 7, the percentage of MKE in the $M_{11} = \langle u_1 \rangle \langle u_1 \rangle /2$ component from $3 < Nt < 30$ decreases with increasing Froude number. This difference is especially stark between the $Fr = 3$ case where M_{11} contains at least 90% of the MKE at all times during the flow evolution and the $Fr = 20$ case where M_{11} contains as little as 10% of the MKE at $Nt = 10$. The large differences in the partition of MKE at early time are not observed in the partition of TKE at equivalent times which suggests that the redistribution of MKE occurs in a manner that does not lead to increased turbulence.

It is interesting to note that while the percentage of mean kinetic energy contained in the M_{22} component increases with Froude number, in absolute terms the value of M_{22}, as well as that of M_{33} is larger in the $Fr = 10$ case than the $Fr = 20$ case at equivalent Nt during $3 < Nt < 30$, see Figure 6(b). Both $Fr = 10$ and $Fr = 20$ are larger than $Fr = 3$. The increase in $\langle M_{22} \rangle$ occurs due to the collapse of the wake in the vertical direction and the corresponding spread in the horizontal direction; it is driven by density differences in the vertical direction and Reynolds stresses. The increased values of M_{22} and M_{33} in the $Fr = 10$ case compared to the $Fr = 20$ case likely occur due to the increased amount of time that the wake is subject to mean diffusion. This suggests that the collapse due to buoyancy is creating internal waves and intrusions into the background which can carry a significant amount of mean kinetic energy as well as turbulent kinetic energy.

Unlike the mean kinetic energy, the turbulent kinetic energy, $TKE = \int_A \langle u_i' u_i' \rangle /2\,dA$, Figure 8, and turbulent potential energy, $TPE = \int_A \langle \rho'^2 \rangle /(2Fr^2)\,dA$ (not shown), do not show the same qualitative differences between cases. TPE and TKE evolve in a consistent manner with a transition in flow regimes between $Nt = 30$ and $Nt = 50$ with the higher Froude number cases transitioning slightly earlier than the $Fr = 3$ case. Similarly, the internal wave flux, $T_p = \int_C \langle p' u_n' \rangle\,dC$ where C denotes the closed curve around the $x_2 - x_3$ boundary (not shown), and turbulent dissipation, $\varepsilon = \langle \partial u_i'/\partial dx_k\, \partial u_i'/\partial dx_k \rangle /Re$, evolve in a consistent manner between cases as shown in Figure 8(b).

By replacing u_1^2 in Equation (1) with $E = \langle u_i \rangle \langle u_i \rangle + \langle u_i' u_i' \rangle$ we can investigate the spread of the wake in terms of kinetic energy. As shown in Figure 9, both the wake width R_{E2} and wake height R_{E3} show a period of initial growth followed by a contraction. After the contraction, R_{E2} stabilizes and begins to grow again as the wake expands in the Q2D regime. R_{E3} continues to decrease until the Q2D regime when it experiences a reduced decay rate. Peak values of R_{E3} and R_{E2} occur at Nt values consistent with transition between flow regimes in TKE, TPE, and T_p.

The timescales on which production and turbulent dissipation are significant shows a clear difference with increasing Froude number resulting in a shorter buoyancy timescale as shown in Figure 10. In the $Fr = 10$ and $Fr = 20$ cases, production ceases to be significant in the first 2 buoyancy periods whereas it is slowly but steadily increasing in the $Fr = 3$ case. Similarly, the turbulent dissipation begins to plateau around $Nt = 10$ for the $Fr = 10$ and $Fr = 20$ cases but steadily grows in the $Fr = 3$ case. It should be noted that the cumulative integral of production is identical for the $Fr = 10$ and $Fr = 20$

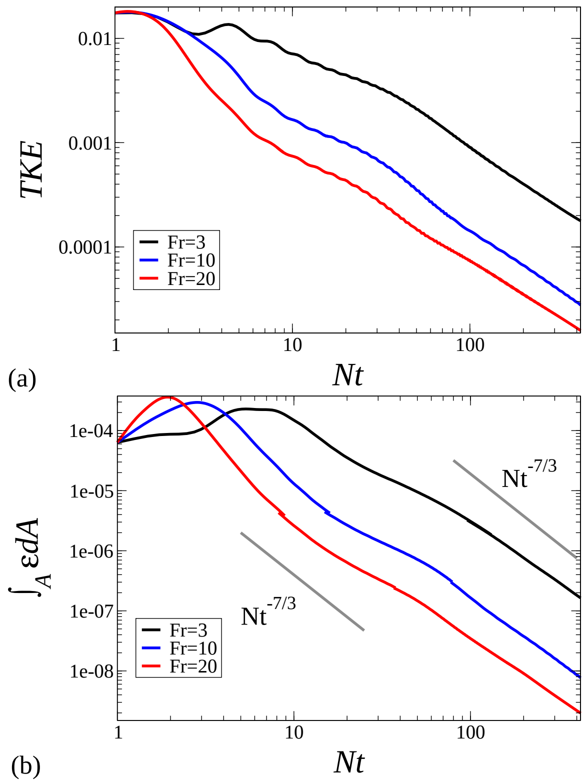

Figure 8: (a) Evolution of integrated turbulent kinetic energy. (b) Evolution of integrated dissipation.

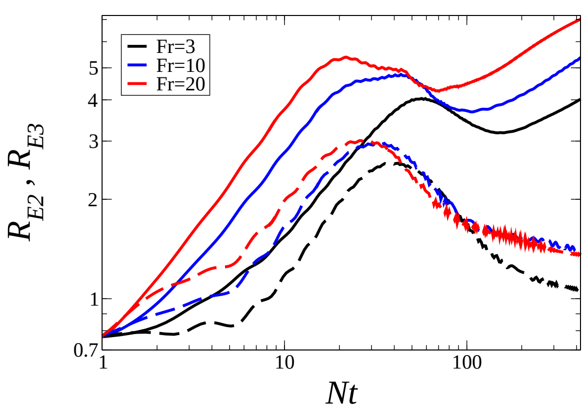

Figure 9: Wake width based on kinetic energy (solid line) and wake height based on kinetic energy (dashed line).

cases and that the cumulative integral of production in the $Fr = 3$ case remains lower at $Nt = 400$ although it is has not plateaued by the conclusion of the simulation. Thus, the decay of MKE (owing to transfer through shear production to TKE) is significantly slower in the $Fr = 3$ case leading to a longer-lived mean wake when the stratification is high. Increased Froude number also results in a significant increase in the amount of turbulent energy lost to turbulent dissipation with differences of $\approx 10\%$ between cases.

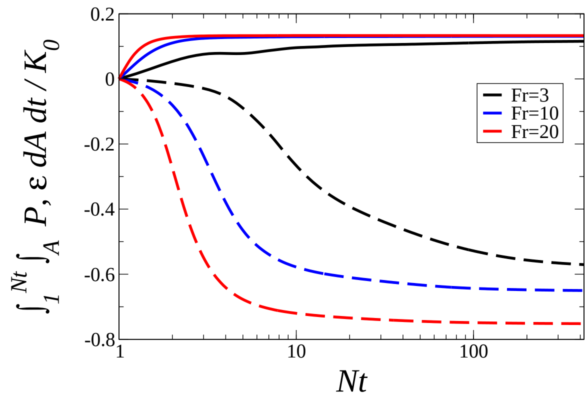

Figure 10: Cumulative integrals of production (solid lines) and dissipation (dashed lines) normalized by the TKE at the beginning of the simulation.

DIFFERENCES IN FLOW STRUCTURE DUE TO FROUDE NUMBER EFFECTS

All cases begin with an identical profile comprised of a doubly-inflected mean streamwise velocity profile with a roughly Gaussian shape to the velocity fluctuations. As the flow evolves the horizontal mean velocity structure is quickly lost within the first 10 buoyancy periods. As the Froude number is increased, the degree of disorder in the mean velocity profile increases significantly at early time and is preserved throughout the evolution of the wake. All cases case quickly transitions to a profile with two drag lobes located above and below a central thrust lobe, these lobes expand and decay as time evolves. Asymmetry is present in all cases with significantly higher levels of asymmetry present in the $Fr = 20$ case.

The turbulent kinetic energy profiles show evidence of layering in the NEQ regime. With increased Fr the mean turbulent kinetic energy appears slightly wider and more rectangular. At late time, the re-adjustment of the turbulent kinetic energy in the NEQ regime results in qualitatively different profiles between cases as shown in Figure 11. The $Fr = 20$ case appears quasi Gaussian with significantly increased horizontal extent. In the $Fr = 10$ case (not shown), the TKE profile appears dominated by two offset peaks at $x_3 = 0$ which appear to correspond to eddies in the late wake. The $Fr = 3$ case shows a three lobed structure with three high aspect ratio structures centered roughly at $x_2 = 0$ and at vertical positions corresponding to the centers of the thrust and drag lobes.

Wakes in stratified fluids are known to develop large, coherent pancake eddies in the late wake. As observed by Diamessis *et al.* (2011), we note that the width of the wake increases with increasing Froude number at equivalent Nt as shown in Figure 12. This difference is most clear when the structures become more coherent at late time, $Nt > 60$. Despite the increased size at higher Fr, the wake structures look qualitatively similar in all cases. Layering in the vertical direction is observed in all cases as coherent vortices emerge at offset vertical and horizontal positions.

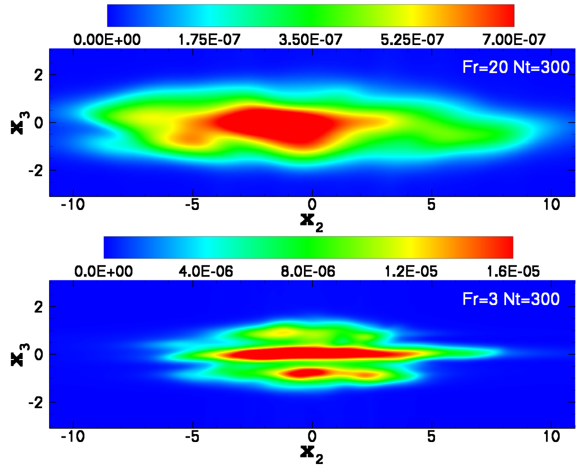

Figure 11: $\langle K \rangle$ at $Nt = 300$. (Top) $Fr = 20$. (Bottom) $Fr = 3$. Contour levels are drawn with the highest level corresponding to $0.7\max(K)$.

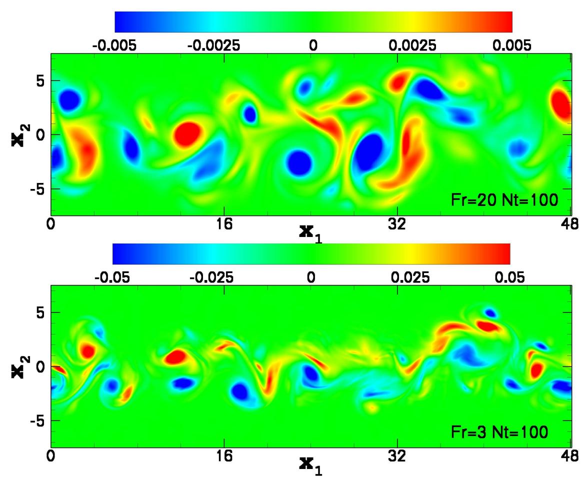

Figure 12: ω_3 at $x_3 = 0$ at $Nt = 100$. (Top) $Fr = 20$. (Bottom) $Fr = 3$. Contour levels are drawn at $\pm\max\omega_3/2$.

CONCLUSIONS

Direct numerical simulation was performed to study the effect of Froude number on a self-propelled wake in a stratified fluid. At increased Froude number, buoyancy effects are delayed which allows the wake to decay faster resulting in smaller values of mean and turbulent statistics such as U_0, MKE, TKE at equivalent Nt. The faster decay of the wake is balanced by increased spread resulting in large wake width and height in cases with increased Fr. The evolution of the wake at different Froude numbers was found to follow qualitatively similar behavior when shown versus Nt despite transition between flow regimes occurring at slightly different Nt between cases. Different scalings were observed for the turbulent and mean velocity statistics which shows that self-similarity is not valid. At higher Fr, the vertical collapse was found to result in intrusions into the background carrying away substantially increased levels of mean kinetic energy through the M_{22} component. These intrusions profoundly change the composition of the mean kinetic energy although these differences in MKE do not result in corresponding differences in TKE.

The flow structure is similar between cases at different Fr although higher levels of asymmetry was observed with increasing Fr. A consistent streamwise velocity structure with two drag lobes located above and below a thrust lobe was observed for all cases. The turbulent kinetic energy showed different profiles at late time with a single peaked structure at $Fr = 20$, a double peaked structure with both peaks occurring at $x_3 = 0$ at $Fr = 10$ and a triple peaked structure with all three peaks occurring close to $x_2 = 0$ at $Fr = 3$. As expected from the calculated wake width, the vorticity field shows that the wake width increases with increasing Fr at equivalent Nt although the strength of the vortices is reduced.

ACKNOWLEDGMENTS

M.B.S. received support on this project from an ARCS Scholarship and an NDSEG Fellowship (HPCMO). M.B.S. and S.S acknowledge the support of the Office of Naval Research (ONR) Grant No. N0014-11-10469, program monitor Ron Joslin. Computational resources were provided by the Department of Defense High Performance Computing Modernization Program. All simulations were run on Diamond, an SGI Altix ICE 8200 LX at the US Army Corps of Engineers Engineering Research and Development Center.

REFERENCES

Brucker, K.A. & Sarkar, S. 2010 A comparative study of self-propelled and towed wakes in a stratified fluid. *J. Fluid Mech.* **652**, 373–404.

Chernykh, G.G., Moshkin, N.P. & Fomina, A.V. 2009 Dynamics of turbulent wake with small excess momentum in stratified media. *Comm. in Nonlinear Sci. and Numerical Simulation* **14**, 1307–1323.

Diamessis, P. J., Spedding, G. R. & Domaradzki, J.A. 2011 Similarity scaling and vorticity structure in high Reynolds number stably stratified turbulent wakes. *J. Fluid Mech.* **671**, 52–95.

Lin, J.T. & Pao, Y.H. 1979 Wakes in stratified fluids. *Ann. Rev. Fluid Mech.* **11**, 317–338.

Meunier, P. & Spedding, G.R. 2006 Stratified propelled wakes. *J. Fluid Mech.* **552**, 229–256.

Riley, James J. & LeLong, Marie-Pascale 2000 Fluid motions in the presence of strong stable stratification. *Ann. Rev. Fluid Mech.* **32**, 613–657.

Rottman, J. W., Dommermuth, D. G., Innis, G. E., O'Shea, T. T. & Novikov, E. 2003 Numerical simulation of wakes in a weakly stratified fluid. *Proceedings of the 24th Symposium on Naval Hydrodynamics* pp. 517–533.

Spedding, G. 1997 The evolution of initially turbulent bluff-body wakes at high internal Froude number. *J. Fluid Mech.* **337**, 283–301.

de Stadler, M.B., Sarkar, S. & Brucker, K.A. 2010 Effect of the Prandtl number on a stratified turbulent wake. *Phys. Fluids* **22** (9), 095102.